NRC Research Press

ARTICLE

A structure-property study toward π-extended phosphole chromophores with ambipolar redox properties

Yi Ren and Thomas Baumgartner

Abstract: We report the synthesis of a series of π-extended dithienophospholes with phenyl or biphenyl terminal groups via Suzuki Miyaura cross-coupling procedures. The incorporation of the dithienophosphole core into the scaffold on oligophenylenes was found to lead to pronounced luminescence properties in solution and the solid state, the latter of which also responded to different solid-state morphologies, i.e., powder versus crystal. More importantly, the investigated molecular architectures also allowed — for the first time — the observation of ambipolar redox behavior of such species, with the biphenyl-extended species in particular showing quasi-reversible reduction *and* oxidation processes; the observed experimental features were correlated with computational density functional theory studies.

Key words: phosphorus heterocycles, conjugated materials, organic electronics, luminescence, electrochemistry, ambipolar redox properties, DFT calculations.

Résumé : Nous présentons la synthèse d'une série de dithiénophospholes à conjugaison π étendue portant des groupes terminaux phényle ou biphényle que nous avons réalisée par couplage croisé de Suzuki Miyaura. Nous avons observé que l'incorporation du noyau dithiénophosphole aux oligophénylènes du squelette donnait lieu à des propriétés de luminescence marquées, en solution et à l'état solide. Par ailleurs, ces propriétés se trouvaient modulées selon différentes morphologies de l'état solide, à savoir la poudre ou le cristal. Fait important, les architectures moléculaires auxquelles nous nous sommes intéressés permettaient également — pour la première fois — d'observer le comportement oxydoréducteur ambipolaire de telles espèces, surtout dans le cas de celles qui étaient étendues grâce aux groupes biphényle, pour lesquelles on observait des processus de réduction *et* d'oxydation quasi-réversibles. Ces caractéristiques observées en conditions expérimentales ont été corroborées par des études de modélisation employant la théorie de la fonctionnelle de la densité. [Traduit par la Rédaction]

Mots-clés : hétérocycles phosphorés, substances conjuguées, électro-organique, luminescence, électrochimie, propriétés d'oxydoréduction ambipolaires, calculs DFT.

Introduction

Organic π-conjugated materials can exhibit intriguing photophysical properties such as high fluorescence quantum yields, charge/energy transfer, and tunable absorption/emission as well as valuable redox behavior and self-organization properties.[1–3] These highly diverse features have attracted significant attention in the area of organic electronics for devices such as organic light-emitting diodes,[1] organic field-effect transistors,[2] and organic photovoltaic cells.[3] In addition, low-cost solution processability of organic π-conjugated materials can be further harnessed to fabricate large area and flexible electronic devices for real-world applications.[4] For the majority of practical applications, it is very important to have a balanced hole and electron injection/transport to achieve good device performance.[5] Along with the development of organic materials, p-type semiconducting materials (hole injection/transport materials) have progressed tremendously. However, n-type semiconducting materials for organic electronics have remained still relatively limited, even to date.[6] Therefore, it is very desirable to design new organic materials with a low lowest unoccupied molecular orbital (LUMO) energy level that can potentially decrease the barrier of electron injection between high work function electrodes and the LUMO energy levels of organic semiconducting materials. To lower the LUMO energy level, it has been demonstrated that introducing strongly electronegative fluoro substituents into well-known hole-transporting materials could induce a strong electron-accepting character and strong intermolecular interactions with enhanced electron-injection/transport features.[5c,7]

Compared to thiophenes and pyrroles, on the other hand, both experimental and theoretical studies revealed that the LUMO energy level of phosphole derivatives is stabilized through σ*–π* orbital coupling.[8] This hyperconjugation makes phosphole-based materials promising electron-acceptor candidates and several articles that have been published by others and us have now established the strong electron-acceptor properties of π-conjugated phosphole materials in general.[9] However, phosphole-based materials that exhibit both electron-accepting *and* electron-donating character evident via ambipolar redox properties have remained elusive to date. Our early studies indicated that the dithienophosphole core itself does not exhibit reversible reduction features.[10] Recent efforts by our group and others involved increasing the π-conjugation of the system that further stabilized the electrochemical reduction features.[11] This article now deals with the corresponding structure-property studies toward phospholes with ambipolar redox properties, using extended π-conjugation to balance the acceptor features of the central dithienophosphole oxide unit, with (bi)phenyl substituents in the 2,6-positions of the scaffold. Our choice of phenyl terminal groups was based on their mildly electron-donating character that would

Received 22 July 2015. Accepted 22 August 2015.

Y. Ren* and T. Baumgartner. Department of Chemistry and Centre for Advanced Solar Materials, University of Calgary, 2500 University Drive NW, Calgary, AB T2N 1N4, Canada.

Corresponding author: Thomas Baumgartner (e-mail: thomas.baumgartner@ucalgary.ca).

*Present address: Department of Chemical and Biological Engineering, Princeton University, Princeton, NJ 08544, USA.

Can. J. Chem. **94**: 1–8 (2016) dx.doi.org/10.1139/cjc-2015-0347

Scheme 1. Synthesis of the π-extended phospholes.

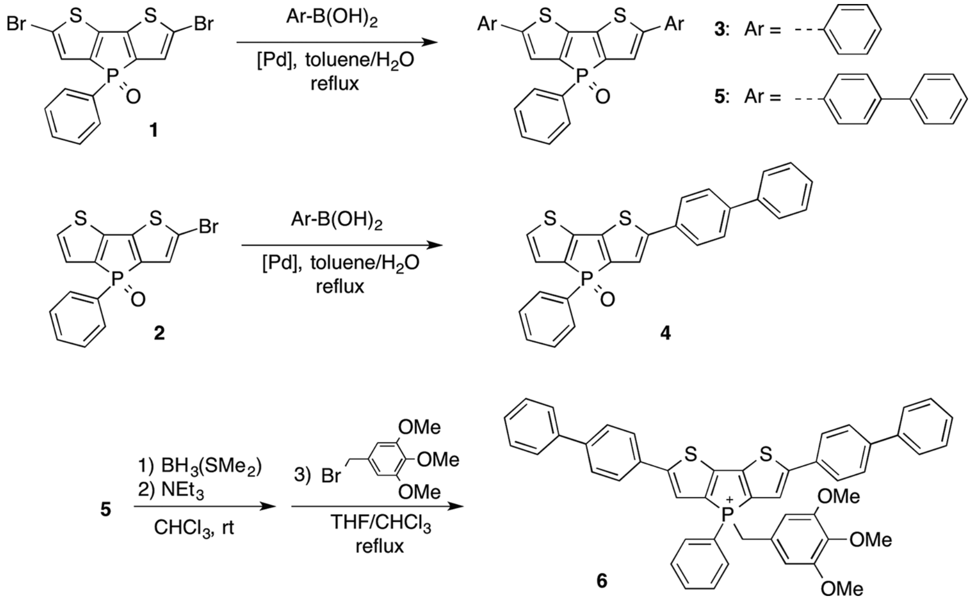

not lead to a strongly pronounced charge-transfer state for the overall conjugated scaffold. Moreover, the presence of torsion angles between the terminal biphenyl rings and the dithienophosphole that potentially limits the conjugation throughout the extended backbone was expected to support a balancing point where it is not only possible to stabilize the reduction process of dithienophosphole core but also to maintain an easy oxidation process of phenyl/biphenyl groups in the (bi)phenyl-substituted phospholes.

To gain a deeper understanding of the evolution of potentially ambipolar redox behavior, we have focused on the systematic extension of the dithienophosphole scaffold via introduction of two (symmetric and asymmetric) and four phenyl rings (symmetric) in the context of this combined experimental and computational study.

Results and discussion

The required mono-/dibromodithienophosphole starting materials **1** and **2** were synthesized according to the procedures reported by our group earlier[10c,12] and subsequently reacted with aryl boronic acid species via Suzuki Miyaura-based protocols to give the target compounds **3**,[10c] **4**, and **5** (Scheme 1). The identity of all new compounds was confirmed by ^{1}H, ^{13}C, and ^{31}P NMR spectroscopy and high-resolution mass spectrometry. Interestingly, the extended phospholes **3**, **4**, and **5** were found to form 1D needle-shaped crystals during slow evaporation of the solvent during the crystallization that were, however, unsuited for single-crystal X-ray crystallography (Fig. 1).

This suggested some self-assembly potential for the new molecular materials, a feature that we have developed in our recent studies via the novel “phosphole-lipids”, which form intriguing liquid-crystal phases as well as stimuli-responsive organogels from hydrocarbon solvents.[13] In the latter, we have utilized the presence of long dodecyloxy chains as well as a charged phosphorus center, which were balanced with the π-stacking interactions of the main conjugated scaffold to give rise to self-assembled nano-/microstructures. We have thus included the phospholium species **6** in this study as well, particularly since the cationic phosphorus center should exhibit a more pronounced electron-acceptor character than the corresponding oxide.[11b] For the synthesis of the cationic congener **6**, oxide species **5** was first reduced to the trivalent phosphole species via procedures also reported by our group[10c] followed by the reaction between the trivalent phosphole and trimethoxybenzyl bromide to afford the cationic benzylated derivative **6** (Scheme 1).[14]

Photophysical properties

The photophysical properties of the extended phosphole oxides are summarized in Table 1. These phosphole species show the expected red-shifted absorption and emission upon extension of the central dithienophosphole core in the order **4** < **3** < **5** (Fig. 2). Notably, upon changing the solvent polarity, the compounds show more pronounced red-shifts in their emission (**3**: λ_{em} = 522 nm in EtOH, λ_{em} = 507 nm in CH_3CN, λ_{em} = 515 nm in $CHCl_3$, λ_{em} = 498 nm in cyclohexane; **4**: λ_{em} = 499 nm in EtOH, λ_{em} = 487 nm in CH_3CN, λ_{em} = 492 in $CHCl_3$; **5**: λ_{em} = 533 nm in EtOH, λ_{em} = 522 nm in CH_3CN, λ_{em} = 528 nm in $CHCl_3$) compared to their absorption maxima (**3**: λ_{abs} = 422 nm in EtOH, λ_{abs} = 423 nm in $CHCl_3$, λ_{abs} = 418 nm in CH_3CN, λ_{abs} = 415 nm in cyclohexane; **4**: λ_{abs} = 402 nm in EtOH, λ_{abs} = 398 nm in CH_3CN, λ_{abs} = 401 in $CHCl_3$; **5**: λ_{abs} = 440 nm in EtOH, λ_{abs} = 434 nm in CH_3CN, λ_{abs} = 438 nm in $CHCl_3$), which can be attributed to a more polarized structure in the excited state.

Phospholium salt **6** exhibits a further red-shifted absorption and emission due to the more polarized phosphonium center arising from its increased acceptor character when compared to its oxide congener **5**. Moreover, the emission spectrum of **6** is also very broad (full width at half-maximum (fwhm) = 94 nm) relative to the oxide derivatives (cf. fwhm = 81 nm for **5**, fwhm = 81 nm for **3**, fwhm = 79 nm for **4**), suggesting a more flexible structure of **6** similar to that found in the related phosphole-lipids and their model compounds.[13,14] Remarkably, the extended phosphole oxide and phospholium compounds show very high quantum yields in $CHCl_3$ (Table 1), with **3** showing the highest quantum yield of ϕ_{FL} = 0.89, which is in line with previously reported π-extended phosphole oxides[10c,10f] and related phosphole-lipids.[13b]

The emission maxima of the thin films of **3**, **4**, **5**, and **6** are red-shifted compared with those of their solutions, probably due to the restricted rotation of the terminal aryl groups and π–π interaction between neighboring molecules in the solid state.[13b,14] The decreased but still considerable fluorescence quantum yields of **3**, **4**, **5**, and **6** in the solid state also indicate that π–π interactions between the molecules quench the fluorescence to some extent. It is worth mentioning that **6** with the bulky trimethoxybenzyl group

Fig. 1. Polarized optical micrographs of the 1D needle-shaped crystals of (*a*) **3**, (*b*) **4**, and (*c*) **5**.

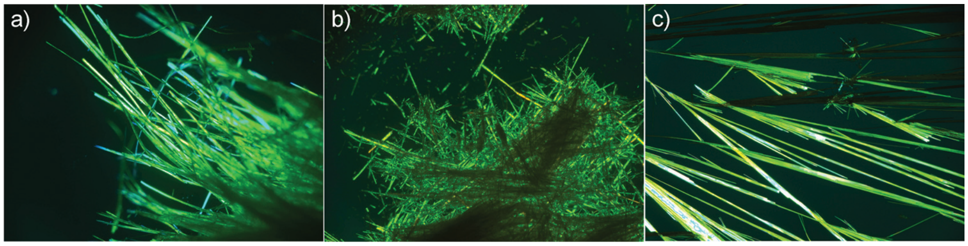

Table 1. Photophysical data of the extended phospholes.

Compound	λ_{abs} (nm)[a], $CHCl_3$	ε (L mol^{-1} cm^{-1})	λ_{em} (nm)[a], $CHCl_3$	ϕ_{FL}[b], $CHCl_3$	Band gap (eV)[c]	λ_{em} (nm)[d], film	λ_{em} (nm), solid	ϕ_{FL}[b], solid
3	423	19 740	515	0.89	2.58	537	555[e]	0.15
4	401	14 700	491	0.51	2.72	508	508[e]	0.28
5	438	29 580	527	0.83	2.49	558	579[f]	0.12
6	456	Not determined	558	0.75	2.38	577	571[g]	0.36

[a] Measured at 10^{-5} mol/L.
[b] Determined by a calibrated integrating sphere system.
[c] Determined from the onset of the absorption.
[d] Drop cast film from $CHCl_3$ solution (10^{-3} mol/L).
[e] 1D needle-shaped crystals.
[f] Solid powders from $CHCl_3$ solution.
[g] Crystals.

Fig. 2. (*a* and *b*) Absorption and emission spectra of the extended phospholes in $CHCl_3$. (*c* and *d*) Emission spectra of **5** (left) and **6** (right) at different states.

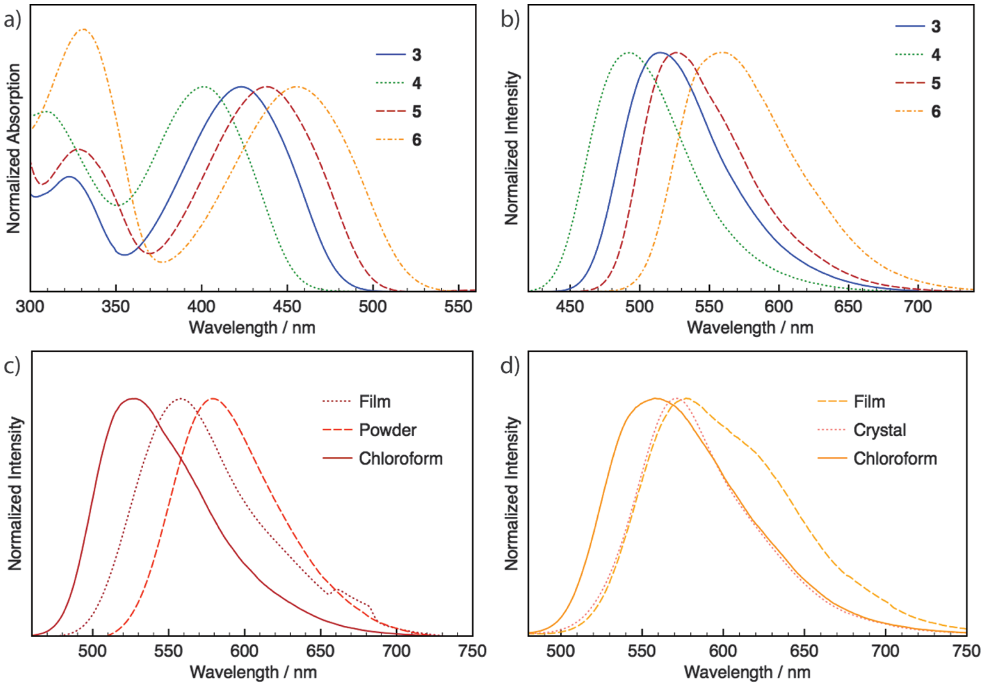

exhibits a relatively higher fluorescence quantum yield compared to the oxide congeners, which is probably due to its propensity to suppress strong π–π stacking.[13b,14]

Interestingly, the extended phospholes also show different emission features in different states. The 1D needle-shaped crystals (λ_{em} = 555 nm) of **3** show a red-shifted emission compared with that of the thin film (λ_{em} = 537 nm). The powder of **5** (λ_{em} = 579 nm) obtained from slow evaporation of $CHCl_3$ exhibits a 20 nm red-shifted emission maximum compared with that of the thin film emission (λ_{em} = 558 nm) (Fig. 2*c*). The thin film emission of **6** (λ_{em} = 577 nm) with the bulky trimethoxybenzyl group is very broad, with a red-shifted shoulder (λ_{em} = 613 nm) compared to its crystal-state emission (λ_{em} = 571 nm) (Fig. 2*d*). Particularly, the broad thin-film emission of **6** strongly suggests the presence of several different isomers (i.e., conformers arising from twisted terminal phenyl groups as well as rotation of the *p*-benzyl substituent),[13,14] which is not the case for its crystal-state emission, resulting from a single 'locked' conformation for the latter.

Electrochemical properties

The electrochemical data are summarized in Table 2. Generally, the extended phosphole oxides show quasi-reversible reduction features (Fig. 3) whose potentials are decreasing upon extension of the central dithienophosphole core (E_{red} = –2.18 V for **4**, –2.08 V for

Table 2. Electrochemistry data of the extended phospholes.

Compound	E_{red} (V)[a]	E_{ox} (V)[a]	Band gap (eV)[d]	EA (eV)[e]	IP (eV)[f]
3	−2.08[b]	0.87[b]	2.59	−2.52	6.01
4	−2.18[b]	0.77[b] 1.09[c]	2.75	−2.42	5.91
5	−2.04[b]	0.75[b] 1.08[b]	2.47	−2.56	5.89
6	−1.56[c]	0.39[c]/0.62[c] 1.02[c]/1.16[d] 1.30[c]	1.66	na	na

Note: Versus Fc/Fc$^+$, measured in CH_2Cl_2 with a platinum rod as the working electrode, platinum wire as a counterelectrode, and Ag/AgCl/KCl (3M) as the reference electrode; the supporting electrolyte was NBu_4PF_6, standard scan rate was 100 mV/s.

[a] $E_{\mathrm{red}}(E_{\mathrm{ox}}) = 1/2(E_{\mathrm{pc}} + E_{\mathrm{pa}})$ for reversible or quasi-reversible process; otherwise, $E_{\mathrm{red}}(E_{\mathrm{ox}}) = E_{\mathrm{pc}}(E_{\mathrm{pa}})$.

[b] Quasi-reversible process.

[c] Irreversible process.

[d] Determined from onset of oxidation/reduction.

[e] Electron affinity.

[f] Ionization potential.

3, −2.04 V for **5** versus Fc/Fc$^+$), in line with the obtained photophysical data. Despite being irreversible, **6**, with the more positive phospholium center, shows a more positive reduction potential at −1.56 V due to a further lowered LUMO energy level, which is consistent with theoretical studies (vide infra). Interestingly, all extended phosphole oxides also exhibit quasi-reversible oxidation processes, which is rarely observed in phosphole-based small conjugated molecules.[11b] It was found that compounds **4** and **5** with the biphenyl terminus usually display similar oxidation processes (first and second oxidation), which are more positive than the oxidation potentials of the phenyl-substituted compound (E_{ox} = 0.87 V for **3**, 0.77/1.09 V for **4**, 0.75/1.08 V for **5** versus Fc/Fc$^+$). This observation indicates that the quasi-reversible oxidation is likely due to the oxidation of terminal aryl groups (phenyl and biphenyl) instead of the phosphole core.

Notably, the electrochemically determined band gaps for the neutral species **3**–**5** (**3**: 2.59 eV; **4**: 2.72 eV; **5**: 2.49 eV) are near perfect matches with the optical band gaps from UV-vis spectroscopy (Table 1). There is, however, a discrepancy between the electrochemically determined and optical band gap for **6**, which can be ascribed to the cationic nature of the species. This may lead to a more complex situation during the cyclic voltammetry (CV), potentially involving the electron-donating trimethoxyphenyl moiety as well, which may also be responsible for the observed irreversible features.

The solid-state electron affinities and ionization potentials of the phosphole oxides were estimated using the electrochemical data (Table 2).[15] The estimated solid-state electron affinity values of **3** and **5** are −2.52 and −2.56 eV, respectively, which are more exothermic than that of aluminum trisquinolate, Alq_3, a popular electron-transport material (approximately −2.3 eV) and closer to C_{60} (approximately −3.7 eV), while the solid-state ionization potential of **5** (5.9 eV) is somewhat higher than that of pentacene, a benchmark p-type semiconductor material at approximately 5.1 eV.[16] Therefore, the current electrochemistry studies suggest that the π-extended phosphole oxides, and particularly **5**, may potentially be suitable candidates for ambipolar semiconducting materials.

Density functional theory (DFT) calculations

To gain some deeper insight into the observed electronic features of the π-extended dithienophospholes, and particularly their electrochemical properties, we have performed DFT calculations at the B3LYP/6-31+G(d) level of theory using the Gaussian03 suite of programs.[17] In this context, we have determined the frontier orbital energies and minimized geometries for the neutral (and cationic in the case of **6**) species (Table 3) as well as their oxidized and reduced congeners (Table 4), including the spin densities of the latter.

The relevant frontier orbitals for all species show the typical distributions for (extended) dithienophospholes (see Fig. 4 for representative species and the Supplementary material section for the complete sets), with the highest occupied molecular orbitals (HOMOs) comprising the π-systems, while the LUMO orbitals represent the corresponding quinoidal π*-systems. HOMO−1 and LUMO+1 also correspond to the π- and π*-systems (with the exception of **6** for which the LUMO+1 largely corresponds to the exocyclic *P*-phenyl group) but have larger contributions from the appended (bi)phenyl substituents. Importantly, the HOMO–LUMO gaps match the trend observed for the species by optical spectroscopy as well as CV (**4**: 3.39 eV > **3**: 3.22 eV > **5**: 3.07 eV > **6**: 2.84 eV) but overestimate the band gaps between 0.5 and 0.7 eV (1.2 eV for **6**; from CV). It should be pointed out in this context that this discrepancy could be attributed to the fact that the DFT-derived values represent the gas phase for **3**, **4**, and **5**, whereas the experimental values have been obtained from solution, which is known to considerably affect the electronics of polar conjugated systems. Moreover, it is now also well established that DFT calculations on conjugated molecules with charge-transfer properties fail to reproduce the energies of the relevant frontier orbitals.[18]

The frontier orbitals for **6** support the increased polarity of the molecular scaffold, suggesting a much more pronounced charge-transfer character for the HOMO → LUMO transition, evident in the considerably more localized LUMO on the dithienophosphole core. Moreover, the LUMO energy level of the cationic **6** is nearly 1 eV lower than that of the other oxide congeners, in line with the experimentally determined photophysics, the reduction potentials, and the ionic nature of the phosphorus center (vide supra). Other important parameters are the torsion angles between the dithienophosphole core and the appended (bi)phenyl termini. It is important to note that each species shows a considerable twist between these elements with torsion angles τ_α being roughly between 24° and 27° (Chart 1), while τ_β is relatively fixed at 36.5° in either direction. It should be noted that the calculations also suggest no preference in direction for the twisting; both possible rotational isomers seem to represent minima on the electronic hypersurface.

To verify the electrochemical features observed via CV, we then proceeded to calculate the minimized structures, orbital energies, and spin density distributions of the oxidized and reduced species of **3**–**5**, respectively.[19] In the case of **5**, we also included the dicationic relative arising from a second oxidation, which was also observed to be quasi-reversible from the CV. The resulting spin densities for the radical cations and anions are shown in Fig. 5 and suggest full delocalization of the respective radicals across the entire π-conjugated scaffold. Also noteworthy is the fact that the spin densities correspond to the respective singly occupied molecular orbitals (SOMOs) of the oxidized/reduced species as well as the related HOMOs (oxidation) and LUMOs (reduction) of the neutral species. While this supports the stability of the radicals and hence the largely quasi-reversible oxidation behavior, it is difficult to derive the deviating *reduction* behavior between the species, as observed by CV. However, when comparing the energy levels of the corresponding SOMOs, it is evident that the SOMO of **4-red** is significantly higher in energy (−1.78 eV) than those of **3-red** and **5-red** at approximately −2.0 eV, indicating that it may be more prone to subsequent decomposition reactions.

It is also important to note that that oxidation of the π-systems resulted in a considerable flattening of the scaffold, evident in torsion angles τ_α ranging from approximately 1° in **4-ox** and 3° in **5-ox** to 11.5° in **3-ox**. In combination with the least reversible oxidation behavior of **3**, this suggests that a biphenyl group with its extended π-system indeed stabilizes the oxidized species much more effectively than a single phenyl substituent. Moreover, τ_α

Fig. 3. Cyclic voltammograms of (*a*) **3**, (*b*) **4**, (*c*) **5**, and (*d*) **6** in CH_2Cl_2 versus Fc/Fc⁺; NBu_4PF_6 as supporting electrolyte, scan rate 100 mV/s.

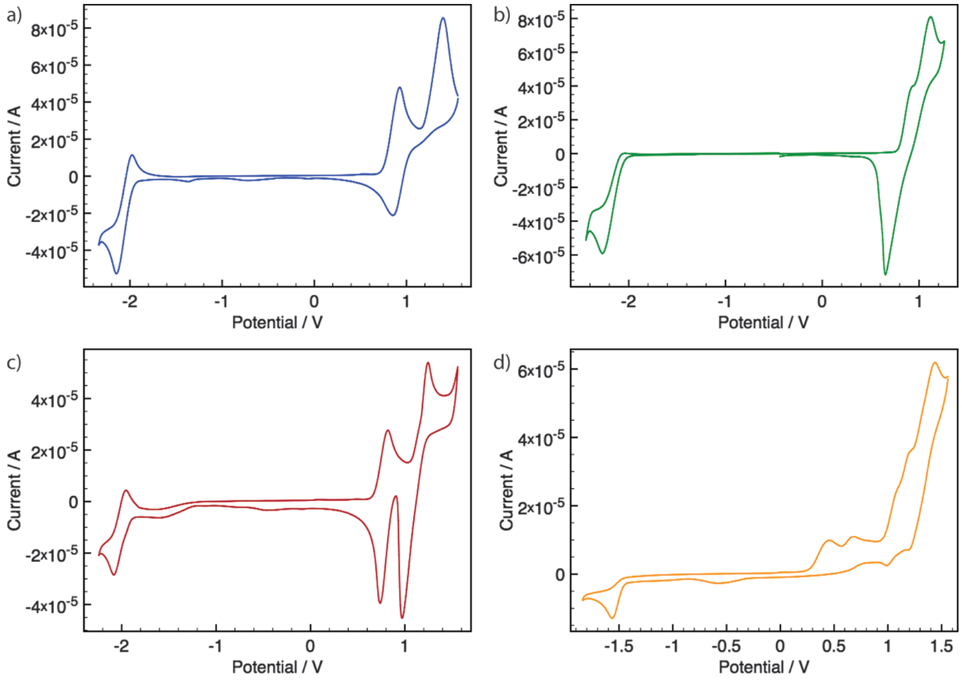

Table 3. Frontier orbital energies (B3LYP/6-31+G(d)) and twist angles of the terminal phenyl substituents of the extended phospholes.

Compound	LUMO+1 (eV)	LUMO (eV)	HOMO (eV)	HOMO–1 (eV)	τ_α (°)[b]	τ_β (°)[b]
3	–0.79	–2.08	–5.30	–6.54	27.0 (1) –27.0 (2)	na
4	–1.00	–2.02	–5.41	–6.40	26.0 (1)	–36.7 (1)
5	–1.15	–2.14	–5.21	–6.08	25.8 (1) 24.8 (2)	–36.5 (1) –36.6 (2)
6[a]	–2.02	–3.11	–5.95	–6.46	27.6 (1) 24.0 (2)	36.5 (1) –36.5 (2)

[a] Calculated using the PCM solvation model (in CH_2Cl_2) to account for omission of anions.

[b] For definition, see Chart 1.

Table 4. Frontier orbital energies (B3LYP/6-31+G(d)) and twist angles of the terminal phenyl substituents of the extended phospholes in their oxidized and reduced states.

Compound	LUMO (eV)[a]	SOMO (eV)[a]	HOMO–1 (eV)[a]	τ_α (°)	τ_β (°)
3-ox	–3.31	–5.63	–7.03	–11.5 (1) 11.5 (2)	na
4-ox	–3.22	–5.60	–7.03	0.79 (1)	–28.1 (1)
5-ox	–3.26	–5.41	–6.48	–3.5 (1) –2.9 (2)	–31.2 (1) –31.1 (2)
5-ox2	–5.64	–6.02[b]	–7.54	–1.6 (1) 0.6 (2)	–23.1 (1) –22.9 (2)
3-red	–0.18	–1.92	–4.14	–0.7 (1) 0.7 (2)	na
4-red	–0.43	–1.78	–4.19	2.9 (1)	–28.0 (1)
5-red	–0.66	–2.04	–4.16	1.5 (1) 2.4 (2)	–30.5 (1) –30.7 (2)

[a] Average of α and β series orbital energies; PCM solvation model (CH_2Cl_2).

[b] Second oxidation occurs from SOMO and the resulting orbital is HOMO.

flattens even more when **5-ox** is oxidized into **5-ox2** (from 3° to 1°), suggesting an even better delocalization of the π-system within the core scaffold in the latter. It should be noted that τ_β is also reduced upon oxidation of the main scaffold, but the effect is much less pronounced with angles ranging from 24° to 32°, suggesting only a minor contribution from the outermost rings for stabilization of the oxidized congeners.

Chart 1. Definition of torsion angles τ_α and τ_β.

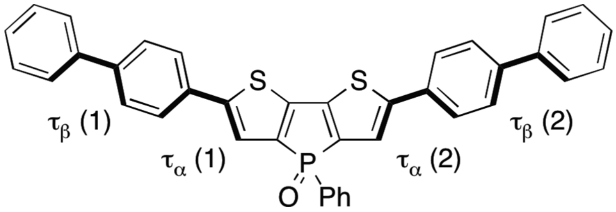

Similarly affected torsion angles are also observed for the corresponding reduced species, with **4-red** (with its irreversible reduction) showing the largest value for τ_α at 2.9°.

Conclusions

In conclusion, we have synthesized a series of (bi)phenyl extended dithienophospholes that are highly luminescent in solution and that also show considerable emissive properties in the solid state. Depending on the molecular geometry and available degrees of rotational freedom in the solid state that determine the morphologies (i.e., crystal versus amorphous film), the solid-state emission can be further tuned over wavelengths of up to 20 nm (for **5**) that suggest high utility of this species as stimuli-responsive solid-state emitters. Moreover, we were able to show that the π-extension of the system triggers electrochemically ambipolar behavior, allowing access to quasi-reversibly stable radical cations and anions, particularly in the case of the symmetrically biphenylated congener **5**. The computationally observed structural changes upon oxidation and reduction of the scaffold as well as the electronic distribution within the HOMO and LUMO orbitals lend support for the phenyl groups being the primary site of oxidation, while the dithienophosphole core is primarily reduced. Once oxidized/reduced, the extended π-system of the scaffold is able to largely stabilize the resulting radicals via delocalization. This is the first example of a highly luminescent dithienophosphole species that shows this amipolar redox behavior. Consequently, this

Fig. 4. Relevant frontier molecular orbitals of compounds **4–6** (B3LYP/6-31+G(d)).

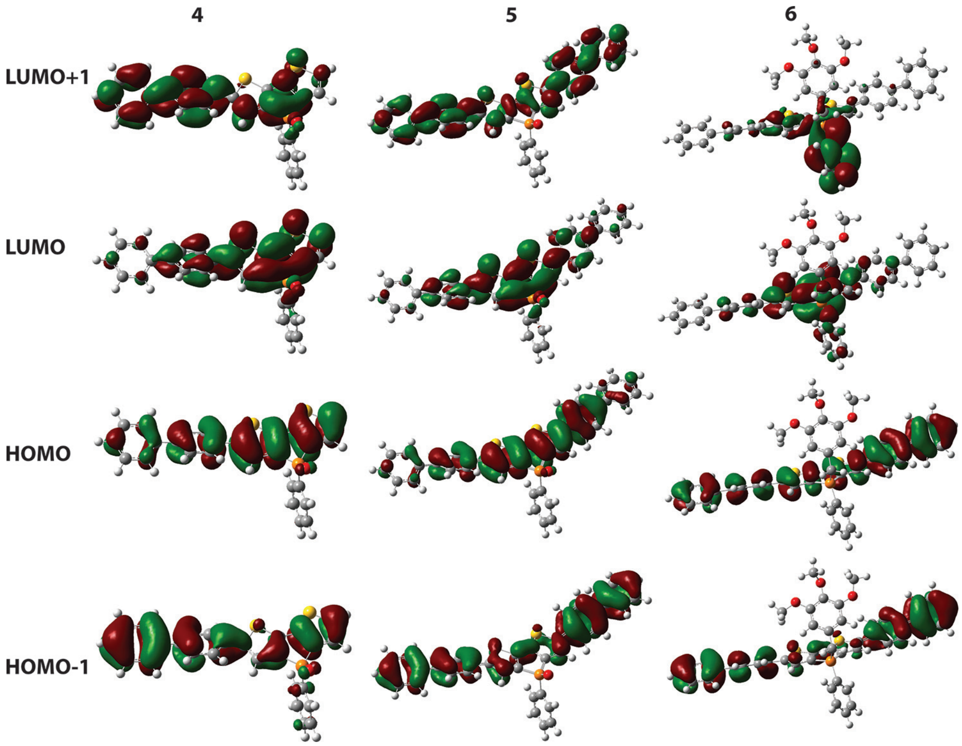

Fig. 5. Spin density distributions (B3LPY/6-31+G(d)) for the oxidized (left) and reduced (right) varieties of compounds **3–5**.

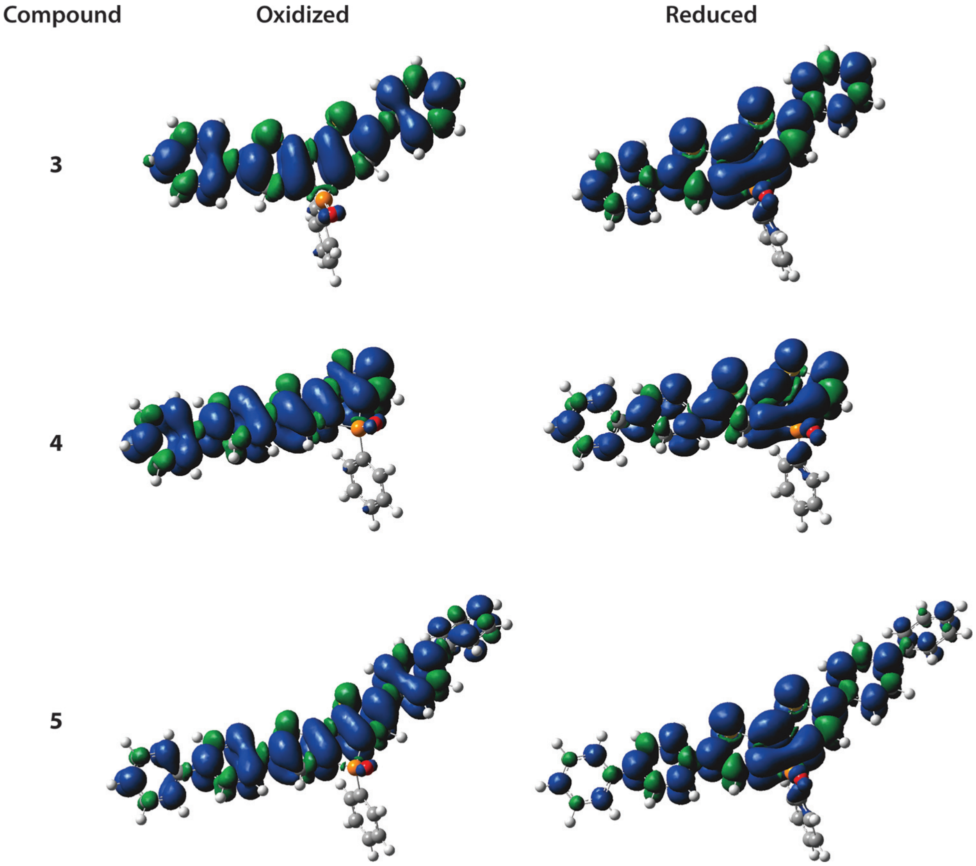

study has provided important insights for the further design of stable ambipolar dithienophospholes for optoelectronic applications and corresponding studies now underway in our laboratory.

Experimental data

General procedures

All manipulations were carried out under a dry nitrogen atmosphere employing standard Schlenk techniques. Solvents were dried using an MBraun solvent purification system. Commercially available chemicals were purchased from Sigma-Aldrich and Alfa-Aesar and were, if not otherwise noted, used as received. 2,6-Dibromodithieno[3,2-*b*:2′,3′-*d*]phosphole oxide **1**[10c] and 2-bromodithieno[3,2-*b*:2′,3′-*d*]phosphole oxide **2**[12] were prepared according to literature procedures. NMR solvents were purchased from Cambridge Isotope Laboratories. $^{31}P\{^{1}H\}$ NMR, ^{1}H NMR, and $^{13}C\{^{1}H\}$ NMR were recorded on Bruker Avance (-II,-III) 400 MHz spectrometers. Chemical shifts were referenced to external 85% H_3PO_4 (^{31}P) and external TMS (^{13}C and ^{1}H). MALDI/TOF and EI mass spectra were run on a Bruker Daltonics AutoFlex III system and Finnigan SSQ 7000 instrument, respectively. All solution fluorescence and UV-vis experiments were recorded on a Jasco FP-6600 spectrofluorometer and UV-Vis-NIR Cary 5000 spectrophotometer. Fluorescence quantum yield and lifetimes were measured by using an Edinburgh Instruments Ltd FLS920P fluorescence spectrometer equipped with an integrating sphere. CV analyses were performed on an Autolab PGSTAT302 instrument with a polished platinum electrode as the working electrode, a platinum wire as counterelectrode, and an Ag/AgCl/KCl3M reference electrode using ferrocene/ferrocenium (Fc/Fc^+) as internal standard. If not otherwise noted, CV experiments were performed in DCM with tetrabutylammonium hexafluorophosphate (0.1 mol/L) as the supporting electrolyte. Theoretical calculations have been carried out at the B3LYP/6-31+G(d) level using the Gaussian03 suite of programs.[17]

General synthetic procedure for 3,[10c] 4, and 5

2,6-Dibromodithienophosphole **1** (1 mmol, 449 mg) or 2-bromodithienophosphole **2** (1 mmol, 376 mg) was added to a toluene water mixture (50 mL, 50:50) of 1 or 2 equiv. of the corresponding boronic acid (phenyl boronic acid or 4-biphenyl boronic acid) in the presence of $Pd(PPh_3)_4$ (5 mol%) and Na_2CO_3. These reaction mixtures were refluxed for 24 h. After removing the solvent under vacuum, the crude products were obtained. The residues were dissolved in $CHCl_3$ and filtered over neutral alumina. Pure compounds **3** (286 mg, 65%),[10c] **4** (317 mg, 72%), and **5** (332 mg, 56%) were obtained via column chromatography (silica, hexane ethyl acetate: from 9:1 to 1:9).

4

^{1}H NMR (400 MHz, CD_2Cl_2): δ = 7.82 – 7.76 (m, 2H), 7.62 – 7.57 (m, 6H), 7.57 – 7.53 (m, 1H), 7.47 – 7.43 (m, 4H), 7.39 – 7.34 (m, 2H), 7.31 (dd, *J* = 8.40 Hz, *J* = 3.2 Hz, 1H), 7.18 (dd, *J* = 4.80 Hz, *J* = 2.4 Hz, 1H) ppm. $^{31}P\{^{1}H\}$ NMR (162 MHz, CD_2Cl_2): 20.3 ppm. $^{13}C\{^{1}H\}$ NMR (100 MHz, $CDCl_3$): δ = 148.0 (d, *J* = 14.3 Hz), 146.1 (d, *J* = 42.2 Hz), 144.1 (d, *J* = 22.9 Hz), 141.2 (s), 140.1 (s), 140.1 (d, *J* = 110.3 Hz), 138.3 (d, *J* = 111.7 Hz), 132.5 (d, *J* = 2.9 Hz), 132.3 (s), 130.9 (d, *J* = 11.3 Hz), 129.7 (d, *J* = 107.3 Hz), 129.0 (s), 128.9 (s), 128.5 (d, *J* = 14.9 Hz), 127.7 (s), 127.6 (s), 126.9 (s), 126.1 (d, *J* = 14.4 Hz), 121.35 (d, *J* = 14.2 Hz) ppm. HRMS (EI-TOF): *m*/*z* = 440.0448 ([M]; calcd. 440.0458).

5

^{1}H NMR (400 MHz, CD_2Cl_2): δ = 7.87 – 7.82 (m, 2H), 7.63 – 7.60 (m, 12H), 7.59 – 7.54 (m, 1H), 7.50 – 7.44 (m, 6H), 7.41 (d, *J* = 2.40 Hz, 2H), 7.37 (tt, *J* = 6.40 Hz, *J* = 1.2 Hz, 1H) ppm. $^{31}P\{^{1}H\}$ NMR (162 MHz, CD_2Cl_2): 20.8 ppm. $^{13}C\{^{1}H\}$ NMR (100 MHz, $CDCl_3$): δ = 148.3(s), 148.1 (s), 144.5 (s), 144.3 (s), 140.7 (d, *J* = 104.0 Hz), 139.4 (d, *J* = 110.9 Hz), 132.6 (d, *J* = 2.7 Hz), 132.3 (s), 130.9 (d, *J* = 11.3 Hz), 129.0 (d, *J* = 13.1 Hz), 128.9 (s), 127.8 (s), 127.7 (s), 126.9 (s), 126.1 (s), 121.5 (d, *J* = 14.3 Hz) ppm. HRMS (MALDI-TOF): *m*/*z* = 593.1166 ([M+H]$^+$; calcd. 593.1157).

6

Compound **6** was obtained by refluxing the reaction mixture of the corresponding trivalent phosphole derivative of **5**, obtained via in situ reduction of **5** (0.34 mmol, 200 mg) via the established procedure,[10c,14] and 3,4,5-trimethoxybenzyl bromide (1.2 equiv., 106 mg) in a toluene THF mixture (30 mL, 40:20) overnight. All solvents were subsequently removed under vacuum and the phospholium bromide salts were purified by column chromatography (silica, hexane ethyl acetate: from 9:1 to 1:9). Yield 131 mg, 51%. ^{1}H NMR (400 MHz, CD_2Cl_2): δ = 8.59 – 8.54 (m, 2H), 8.39 (d, *J* = 2.00, 2H), 7.75 – 7.73 (m, 4H), 7.69 – 7.67 (m, 9H), 7.65 – 7.62 (m, 9H), 7.50 – 7.46 (m, 4H), 7.42 – 7.37 (m, 2H), 6.56 (d, *J* = 3.20 Hz, 2H), 5.28 (d, *J* = 14.8 Hz, 2H), 3.76 (s, 3H), 3.58 (s, 6H) ppm. $^{31}P\{^{1}H\}$ NMR (162 MHz, CD_2Cl_2): 20.0 ppm. $^{13}C\{^{1}H\}$ NMR (100 MHz, $CDCl_3$): δ = 153.1 (d, *J* = 4.5 Hz), 150.3 (d, d, *J* = 14.9 Hz), 147.5 (d, d, *J* = 12.6 Hz), 142.2 (s), 139.8 (s), 135.2 (d, *J* = 3.2 Hz), 134.3 (d, *J* = 11.8 Hz), 131.1 (s), 130.2 (d, *J* = 13.6 Hz), 129.30 (s), 128.0 (s), 127.9 (s), 127.0 (s), 126.6,[6] 126.2 (d, *J* = 96.7 Hz), 124.1 (d, *J* = 14.0 Hz), 122.1 (d, *J* = 10.3 Hz), 115.5 (d, *J* = 83.4 Hz), 107.7 (d, *J* = 6.5 Hz), 60.9 (s), 56.2 (s), 29.7 (s) ppm. HRMS (MALDI-TOF): *m*/*z* = 757.1971 ([M–Br^-]$^+$; calcd. 757.1994).

Supplementary material

Supplementary material is available with the article through the journal Web site at http://nrcresearchpress.com/doi/suppl/10.1139/cjc-2015-0347.

Acknowledgements

Financial support by NSERC of Canada and the Canada Foundation for Innovation is gratefully acknowledged. Y.R. thanks Alberta Ingenuity now part of Alberta Innovates - Technology Futures as well as Talisman Energy for graduate scholarships.

References

(1) (a) Perepichka, I. F.; Perepichka, D. F.; Meng, H.; Wudl, F. *Adv. Mater.* **2005**, *17*, 2281. doi:10.1002/adma.200500461; (b) *Organic Light Emitting Devices*; Müllen, K.; Scherf, U., Eds.; Wiley-VCH: Weinheim, 2006; (c) Veinot, J. G. C.; Marks, T. *J. Acc. Chem. Res.* **2005**, *38*, 632. doi:10.1021/ar030210r; (d) *Organic Electronics*; Klauk, H., Eds.; Wiley-VCH: Weinheim, 2006.

(2) (a) Dimitrakopoulos, C. D.; Malenfant, P. R. L. *Adv. Mater.* **2002**, *14*, 99. doi:10.1002/1521-4095(20020116)14:2<99::AID-ADMA99>3.0.CO;2-9; (b) Allard, S.; Forster, M.; Souharce, B.; Thiem, H.; Scherf, U. *Angew. Chem. Int. Ed.* **2008**, *47*, 4070. doi:10.1002/anie.200701920; (c) Anthony, J. E. *Chem. Rev.* **2006**, *106*, 5028. doi:10.1021/cr050966z; (d) Anthony, J. E. *Angew. Chem. Int. Ed.* **2007**, *46*, 2. doi:10.1002/anie.200790005; (e) Di, C.-A.; Liu, Y.; Yu, G.; Zhu, D. *Acc. Chem. Res.* **2009**, *42*, 1573. doi:10.1021/ar9000873; (f) Klauk, H. *Chem. Soc. Rev.* **2010**, *39*, 2643. doi:10.1039/b909902f; (g) Nelson, T. L.; Young, T. M.; Liu, J.; Mishra, S. P.; Belot, J. A.; Balliet, C. L.; Javier, A. E.; Kowalewski, T.; McCullough, R. D. *Adv. Mater.* **2010**, *22*, 4617. doi:10.1002/adma.201001599.

(3) (a) Günes, S.; Neugebauer, H.; Sariciftci, N. S. *Chem. Rev.* **2007**, *107*, 1324. doi:10.1021/cr050149z; (b) Chen, J.; Cao, Y. *Acc. Chem. Res.* **2009**, *42*, 1709. doi:10.1021/ar900061z; (c) Kippelen, B.; Brédas, J.-L. *Energy Environ. Sci.* **2009**, *2*, 251. doi:10.1039/b812502n; (d) Roncali, J. *Acc. Chem. Res.* **2009**, *42* (11), 1719. doi:10.1021/ar900041b; (e) Mishra, A.; Bäuerle, P. *Angew. Chem. Int. Ed.* **2011**, *51*, 2020. doi:10.1002/anie.201102326; (f) Beaujuge, P.; Fréchet, J. M. J. *J. Am. Chem. Soc.* **2011**, *133*, 20009. doi:10.1021/ja2073643.

(4) (a) Sirringhaus, H.; Kawase, T.; Friend, R. H.; Shimoda, T.; Inbasekaran, M.; Wu, W.; Woo, E. P. *Science* **2000**, *290*, 2123. doi:10.1126/science.290.5499.2123; (b) Rogers, J. A.; Bao, Z.; Baldwin, K.; Dodabalapur, A.; Crone, B.; Raju, V. R.; Kuck, V.; Katz, H.; Amundson, K.; Ewing, J.; Drzaic, P. *Proc. Natl. Acad. Sci. U.S.A.* **2001**, *98*, 4835. doi:10.1073/pnas.091588098; (c) Stutzmann, N.; Friend, R. H.; Sirringhaus, H. *Science* **2003**, *299*, 1881. doi:10.1126/science.1081279; (d) Loo, Y.-L. *AIChE J.* **2007**, *53*, 1066. doi:10.1002/aic.11151.

(5) (a) Murphy, A. R.; Fréchet, J. M. J. *Chem. Rev.* **2007**, *107*, 1066. doi:10.1021/cr0501386; (b) Grimsdale, A. C.; Chan, K. L.; Martin, R. E.; Jokisz, P. G.; Holmes, A. B. *Chem. Rev.* **2009**, *109*, 897. doi:10.1021/cr000013v; (c) Anthony, J. E.; Facchetti, A.; Heeney, M.; Marder, S. R.; Zhan, X. W. *Adv. Mater.* **2010**, *22*, 3876. doi:10.1002/adma.200903628; (d) Shirota, Y.; Kageyama, H. *Chem. Rev.* **2007**, *107*, 953. doi:10.1021/cr050143+.

(6) Stolar, M; Baumgartner, T. *Phys. Chem. Chem. Phys.* **2013**, *15*, 9007. doi:10.1039/c3cp51379c.

(7) (a) Usta, H.; Facchetti, A.; Marks, T. J. *Acc. Chem. Res.* **2011**, *44*, 501. doi:10.1021/ar200006r; (b) Yoon, M. H.; Facchetti, A.; Stern, C. E.; Marks, T. J. *J. Am. Chem.*

Soc. **2006**, *128*, 5792. doi:10.1021/ja060016a; (c) Sakamoto, Y.; Suzuki, T.; Kobayashi, M.; Gao, Y.; Fukai, Y.; Inoue, Y.; Sato, F.; Tokito, S. *J. Am. Chem. Soc.* **2004**, *126*, 8138. doi:10.1021/ja0476258.

(8) (a) Baumgartner, T. *Acc. Chem. Res.* **2014**, *47*, 1613. doi:10.1021/ar500084b; (b) Fukazawa, A.; Yamaguchi, S. *Chem. Asian J.* **2009**, *15*, 1386. doi:10.1002/asia.200900179; (c) Baumgartner, T.; Réau, R. *Chem. Rev.* **2006**, *106*, 4681. doi:10.1021/cr040179m.

(9) (a) Stolar, M.; Borau-Garcia, J.; Toonen, M.; Baumgartner, T. *J. Am. Chem. Soc.* **2015**, *137*, 3366. doi:10.1021/ja513258j; (b) Takeda, Y.; Nishida, T.; Minakata, S. *Chem. Eur. J.* **2014**, *20*, 10266. doi:10.1002/chem.201403735; (c) Stolar, M.; Baumgartner, T. *Chem. Asian J.* **2014**, *9*, 1212. doi:10.1002/asia.201301670; (d) Matano, Y.; Ohkubo, H.; Honsho, Y.; Saito, A.; Seki, S.; Imahori, H. *Org. Lett.* **2013**, *15*, 932. doi:10.1021/ol4000982; (e) He, X.-M.; Baumgartner, T. *RSC Adv.* **2013**, *3*, 11334. doi:10.1039/c3ra40286j; (f) Worch, J. C.; Chirdon, D. N.; Maurer, A. B.; Qiu, Y.; Geib, S. J.; Bernhard, S.; Noonan, K. J. T. *J. Org. Chem.* **2013**, *78*, 7462. doi:10.1021/jo400947u; (g) Ren, Y.; Baumgartner, T. *Dalton Trans.* **2012**, *41*, 7792. doi:10.1039/c2dt00024e; (h) Durben, S.; Baumgartner, T. *Inorg. Chem.* **2011**, *50*, 6823. doi:10.1021/ic200951x; (i) Washington, M. P.; Payton, J. L.; Simpson, M. C.; Protasiewicz, J. D. *Organometallics* **2011**, *30*, 1975. doi:10.1021/om200014f; (j) Bruch, A.; Fukazawa, A.; Yamaguchi, E.; Yamaguchi, S.; Studer, A. *Angew. Chem. Int. Ed.* **2011**, *50*, 12094. doi:10.1002/anie.201104114; (k) Tsuji, H.; Sato, K.; Sato, Y.; Nakamura, E. *J. Mater. Chem.* **2009**, *19*, 3364. doi:10.1039/b906197e.

(10) (a) Baumgartner, T.; Neumann, T.; Wirges, B. *Angew. Chem. Int. Ed.* **2004**, *43*, 6197. doi:10.1002/anie.200461301; (b) Durben, S.; Dienes, Y.; Baumgartner, T. *Org. Lett.* **2006**, *8*, 5893. doi:10.1021/ol062580w; (c) Dienes, Y.; Durben, S.; Kárpáti, T.; Neumann, T.; Englert, U.; Nyulászi, L.; Baumgartner, T. *Chem. Eur. J.* **2007**, *13*, 7487. doi:10.1002/chem.200700399; (d) Baumgartner, T.; Bergmans, W.; Kárpáti, T.; Neumann, T.; Nieger, M.; Nyulászi, L. *Chem. Eur. J.* **2005**, *11*, 4687. doi:10.1002/chem.200500152; (e) Dienes, Y.; Eggenstein, M.; Neumann, T.; Englert, U.; Baumgartner, T. *Dalton, Trans.* **2006**, 1424. doi:10.1039/B509277A; (f) Romero-Nieto, C.; Baumgartner, T. *Synlett* **2013**, *24*, 920. doi:10.1055/s-0032-1317804.

(11) (a) Fukazawa, A.; Hara, M.; Son, T.; Okamoto, E.-C.; Xu, C.; Tamao, K.; Yamaguchi, S. *Org. Lett.* **2008**, *10*, 913. doi:10.1021/ol7030608; (b) Dienes, Y.; Eggenstein, M.; Kárpáti, T.; Sutherland, T. C.; Nyulászi, L.; Baumgartner, T. *Chem. Eur. J.* **2008**, *14*, 9878. doi:10.1002/chem.200801549; (c) Linder, T.; Sutherland, T. C.; Baumgartner, T. *Chem. Eur. J.* **2010**, *14*, 7101. doi:10.1002/chem.201000382; (d) Durben, S.; Baumgartner, T. *Inorg. Chem.* **2011**, *50*, 6823. doi:10.1021/ic200951x; (e) Matano, Y.; Saito, A.; Fukushima, T.; Tokudome, Y.; Suzuki, F.; Sakamaki, D.; Kaji, H.; Ito, A.; Tanaka, K.; Imahori, H. *Angew. Chem. Int. Ed.* **2011**, *50*, 8016. doi:10.1002/anie.201102782; (f) Joly, D.; Tondelier, D.; Deborde, V.; Delaunay, W.; Thomas, A.; Bhanuprakash, K.; Geffroy, B.; Hissler, M.; Réau, R. *Adv. Funct. Mater.* **2012**, *22*, 567. doi:10.1002/adfm.201102005.

(12) Durben, S.; Linder, T.; Baumgartner, T. *New J. Chem.* **2010**, *34*, 1585. doi:10.1039/c0nj00026d.

(13) (a) Ren, Y.; Kan, W. H.; Henderson, M. A.; Bomben, P. G.; Berlinguette, C. P.; Thangadurai, V.; Baumgartner, T. *J. Am. Chem. Soc.* **2011**, *133*, 17014. doi:10.1021/ja206784f; (b) Ren, Y.; Kan, W. H.; Thangadurai, V.; Baumgartner, T. *Angew. Chem. Int. Ed.* **2012**, *51*, 3964. doi:10.1002/anie.201109205.

(14) Ren, Y.; Baumgartner, T. *Inorg. Chem.* **2012**, *51*, 2669. doi:10.1021/ic2026335.

(15) (a) Anderson, J. D.; McDonald, E. M.; Lee, P. A.; Anderson, M. L.; Ritchie, E. L.; Hall, H. K.; Hopkins, T.; Nash, E. A.; Wang, J.; Padias, A.; Thayumanavan, S.; Barlow, S.; Marder, S. R.; Jabbour, G.; Shaheen, S.; Kippelen, B.; Peyghambarian, N.; Wightman, R. M.; Armstrong, N. R. *J. Am. Chem. Soc.* **1998**, *120*, 9646. doi:10.1021/ja980707+; (b) Hreha, R. D.; George, C. P.; Haldi, A.; Domercq, B.; Malagoli, M.; Barlow, S.; Brédas, J.-L.; Kippelen, B.; Marder, S. R. *Adv. Funct. Mater.* **2003**, *13*, 967. doi:10.1002/adfm.200304464.

(16) Cahen, D.; Kahn, A. *Adv. Mater.* **2003**, *15*, 271. doi:10.1002/adma.200390065.

(17) Frisch, M. J.; Trucks, G. W.; Schlegel, H. B.; Scuseria, G. E.; Robb, M. A.; Cheeseman, J. R.; Montgomery, J. A., Jr.; Vreven, T.; Kudin, K. N.; Burant, J. C.; Millam, J. M.; Iyengar, S. S.; Tomasi, J.; Barone, V.; Mennucci, B.; Cossi, M.; Scalmani, G.; Rega, N.; Petersson, G. A.; Nakatsuji, H.; Hada, M.; Ehara, M.; Toyota, K.; Fukuda, R.; Hasegawa, J.; Ishida, M.; Nakajima, T.; Honda, Y.; Kitao, O.; Nakai, H.; Klene, M.; Li, X.; Knox, J. E.; Hratchian, H. P.; Cross, J. B.; Bakken, V.; Adamo, C.; Jaramillo, J.; Gomperts, R.; Stratmann, R. E.; Yazyev, O.; Austin, A. J.; Cammi, R.; Pomelli, C.; Ochterski, J. W.; Ayala, P. Y.; Morokuma, K.; Voth, G. A.; Salvador, P.; Dannenberg, J. J.; Zakrzewski, V. G.; Dapprich, S.; Daniels, A. D.; Strain, M. C.; Farkas, O.; Malick, D. K.; Rabuck, A. D.; Raghavachari, K.; Foresman, J. B.; Ortiz, J. V.; Cui, Q.; Baboul, A. G.; Clifford, S.; Cioslowski, J.; Stefanov, B. B.; Liu, G.; Liashenko, A.; Piskorz, P.; Komaromi, I.; Martin, R. L.; Fox, D. J.; Keith, T.; Al-Laham, M. A.; Peng, C. Y.; Nanayakkara, A.; Challacombe, M.; Gill, P. M. W.; Johnson, B.; Chen, W.; Wong, M. W.; Gonzalez C.; Pople, J. A. *Gaussian 03, Revision E.01*; Gaussian Inc.: Wallingford, CT, 2007.

(18) (a) Dev, P.; Agrawal, S.; English, N. J. *J. Chem. Phys.* **2012**, *136*, 224301. doi:10.1063/1.4725540; (b) Karolewski, A.; Stein, T.; Baer, R.; Kummel, S. *J. Chem. Phys.* **2011**, *134*, 151101. doi:10.1063/1.3581788; (c) Reimers, J. R.; Cai, Z.-L.; Bilić, A.; Hush, N. S. *Ann. N. Y. Acad. Sci.* **2003**, *1006*, 235. doi:10.1196/annals.1292.017.

(19) Unfortunately, all attempts to obtain meaningful results for the oxidized and reduced varieties of **6** failed, as neither calculation successfully converged to a minimum.